Fabrication of Highly Antireflective Silicon Surfaces with Superhydrophobicity

Meiwen Cao,[†] Xiaoyan Song,[†] Jin Zhai,[‡] Jinben Wang,[†] and Yilin Wang*[,†]

Key Laboratory of Colloid and Interface Science and Key Laboratory of Organic Solids, Institute of Chemistry, Chinese Academy of Sciences, Beijing 100080, People's Republic of China

Received: March 6, 2006; In Final Form: April 28, 2006

Highly antireflective porous silicon surfaces with superhydrophobicity were obtained by means of chemical etching and fluoroalkylsilane self-assembly. The results show that wettability and reflectivity of these surfaces strongly depend on the etching method and the resultant surface morphology. All of the four resultant porous silicon surfaces by alkaline etching, acidic etching, thick Pt-assisted acidic etching, and thin Pt-assisted acidic etching can reduce reflectance, but the efficiency differs greatly. Except for the alkaline etching, the porous silicon surfaces produced by the other three etching methods can reach superhydrophobicity after fluoroalkylsilane modification. These differences are due to the different surface morphology and roughness. Moreover, the porous silicon surface produced by thin Pt-assisted acidic etching presents abundant holes and particles with diameters ranging from nanometers to submicrometers. This morphology enables the porous silicon surface to own a very low reflectance value that is averaged to be about 3% over the whole experimental photon wavelength spanning 300−800 nm.

Introduction

Wettability of a solid surface is a characteristic property of materials and is controlled by both surface chemical composition and surface topology. A highly hydrophobic surface on which the water contact angle is larger than 150° is commonly called a superhydrophobic surface. To reach superhydrophobicity, a combination of surface roughness and low surface energy is required.[1−4] A superhydrophobic surface has self-cleaning properties and has wide applications in many fields. In recent years, various methods for fabricating superhydrophobic surfaces have been investigated.[5−12]

Antireflectivity of the superhydrophobic surfaces is also very important for their applications such as coatings for optical devices and photovoltaics. Antireflective coatings on surfaces not only can improve the transparency of optical devices through improving the light transmittance ratio[13−19] but also can improve the photovoltaic conversion efficiency of solar cell materials by distorting the wavefront of the radiation to obtain light trapping by total internal reflection inside the surfaces.[20−22] Normally, high antireflectivity is exhibited on the textured and highly porous surfaces. From the viewpoint of surface roughness, superhydrophobicity is competitive with antireflectivity because the surface structures larger than 400 nm would become a scattering source of light.[15,23] Therefore, control of surface roughness is required to satisfy both superhydrophobicity and antireflectivity.

Great effort has been devoted to fabricate superhydrophobic antireflective films during the past several years. Nakayama and co-workers[12,23] developed a method for producing transparent superhydrophobic films. They used a sublimable pore-forming material to provide surface roughness and subsequently coated the surface with fluoroalkylsilane. Yabu et al.[15] prepared the transparent superhydrophobic films by introducing the honeycomb-patterned films of fluorinated polymers and controlling the pore sizes in the subwavelength region. Fujishima and co-workers[24] reported the combination of antireflection and self-cleaning properties in a core−shell-like SiO_2−TiO_2 particle coating by a simple electrostatic attraction method. Additionally, Minami and co-workers,[25] Shang et al.,[16] and Xu et al.[26] have obtained antireflective films with water repellence by the sol−gel method. In their studies, boehmite or silica-based films with controlled roughness were prepared first and then they were coated with low surface energy materials. However, all of these methods require the surfaces to be coated with polymer or inorganic materials and the possible coating materials are limited.

In the present study, we have successfully fabricated porous silicon surfaces with both high antireflectivity and superhydrophobicity by a combination of chemical etching and alkylsilane self-assembly. The most satisfied porous silicon surface presents a water contact angle of larger than 155° and an average reflective loss as low as 3% over the photon wavelengths spanning 300−800 nm.

Experimental Section

Materials. The polished silicon (100) wafers were purchased from the General Research Institute for Nonferrous Metals. Before use, they were ultrasonicated in detergent solution and acetone for 30 min, respectively. Then, the substrates were rinsed thoroughly with water and dried with a nitrogen stream. Fluorooctylmethyldimethoxysilane ($CF_3(CF_2)_5CH_2CH_2Si(OCH_3)$-$CH_3$) (FODMS) was purchased from Matrix Scientific and used as received. Hydrophobically modified poly(acrylamide) (PAM-C12-2%) was prepared using the typical procedure as reported previously,[27] and its average molecular weight (M_w) is ∼200 000.

Fabrication of Porous Silicon Surfaces. First, clean silicon (100) wafers were wet-etched by different methods to produce porous silicon surfaces. These etching methods include (i) etching in NaOH (20%)/PAM-C12-2% (2%) (V/V = 3:1)

* To whom correspondence should be addressed. E-mail: yilinwang@iccas.ac.cn.
[†] Laboratory of Colloid and Interface Science.
[‡] Laboratory of Organic Solids.

10.1021/jp061373a CCC: $33.50
Published on Web 06/14/2006

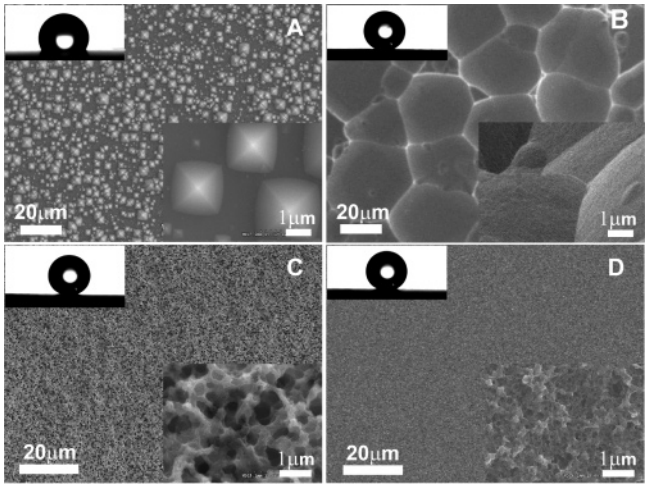

Figure 1. SEM micrographs of the porous silicon surface structures constructed by different etching methods: (A) alkaline etching; (B) acidic etching; (C) thick Pt-assisted acidic etching; (D) thin Pt-assisted acidic etching. The insets are their corresponding magnified images. The water contact angles on these FODMS-modified surfaces were (A) 116°, (B) 153°, (C) 161°, and (D) 155°, respectively.

solution for 3 h (named as alkaline etching), (ii) etching in HF (40%)/HNO_3 (50%)/EtOH (98%) (V/V/V = 1:1:1) solution for 30 s (named as acidic etching), (iii) acidic etching as (ii) after depositing ~20 nm thick platinum (Pt) film on the silicon wafer (named as thick Pt-assisted acidic etching), and (iv) acidic etching as (ii) after depositing ~5 nm thick Pt film on the silicon wafer (named as thin Pt-assisted acidic etching). The Pt films with different thicknesses were comprised of Pt particles with different diameters, and they were sputtered on the silicon wafers using the high vacuum sputtering system (Hitachi, IB-3) by controlling the sputtering time.

Modification of Porous Silicon Surfaces. After chemical etching, the silicon wafers were washed and treated with piranha solution (mixture of H_2SO_4 (98%) and H_2O_2 (30%) at V/V = 7:3) at 80 °C for 1 h to produce a thin oxide layer on the surfaces. Then, the etched surfaces were modified with FODMS precursor using the chemical vapor deposition (CVD) method as reported previously.[28]

Surface Characterization. The morphology of the porous silicon surfaces was observed with scanning electron microscopy (SEM, JEOL JSM 6700F). The composition of the treated surfaces was studied by X-ray photoelectron spectroscopy (XPS, VG ESCALAB MKII spectrometer) with an Al Kα monochromatic X-ray source. Contact angle measurements were carried out with a 2 mg water drop using an optical contact angle meter (Dataphysics Inc, OCA20). The contact angle values reported are averages of at least three measurements made on different areas of the same sample. All measurements for all of the surfaces were within ±2.0° of the averages. The reflectance of the porous silicon surfaces was measured with a UV−vis spectrophotometer (Hitachi model U-3010) equipped with an integrating sphere attachment (Hitachi, 60 mm DIA).

Results and Discussion

Surface Morphologies Produced by Different Etching Methods. As shown in Figure 1, observed by SEM, the porous silicon surfaces show different morphologies after they are treated with different etching methods and modified with FODMS. Alkaline etching on silicon produces a surface with a great amount of pyramids in random sizes (Figure 1A). The sizes of these pyramids are in the range of hundreds of nanometers to several micrometers. From the magnified image, we can see that the sides of the pyramids are smooth and no secondary structures can be found. Differently, the porous silicon surface produced by acidic etching (Figure 1B) presents many pores with large sizes of 10−40 μm in both radius and depth. The walls of these pores are also smooth. However, the porous silicon surfaces generated by either thick or thin Pt-assisted acidic etching show highly porous, spongelike structures (Figure 1C and D). They both present many deep holes and silicon particles that can be graded into different sizes. The sizes of these holes and particles range from nanometers to micrometers for the porous silicon surface produced by thick Pt-assisted acidic etching, while they are obviously smaller and only at the nanometer to submicrometer range for the porous silicon surface produced by thin Pt-assisted acidic etching.

The etching mechanisms of silicon by alkali and acid are described by the following equations (eqs 1[29] and 2[30]):

$$2Si + 2NaOH + 4H_2O \rightarrow Na_2Si(OH)_6 + 2H_2 \quad (1)$$

$$3Si + 18HF + 4HNO_3 \rightarrow 3H_2SiF_6 + 4NO + 8H_2O \quad (2)$$

The alkaline etching of silicon is anisotropic; that is to say, the etching at different silicon planes has different etch rates. This anisotropic behavior has been attributed to the orientation dependence of the kinetics of silicon dissolution[31] or different passivation potentials.[32] Thus, alkaline etching will produce pyramid-like structures on the silicon surface and one etching plane crosses the surface at a fixed angle.[33] The properties of hydrophobically modified polymers are similar to those of surfactants in many ways, such as their self-assembling properties[27] and ability to lower surface energy. Hence, the role of PAM-C12-2% in the alkaline etching might be similar to that of surfactants, which are supposed to occupy the solid−etchant interface, influence the reaction mechanism, and change the anisotropy.[34] Differently, the acidic etching of silicon has no orientation dependence. This etching is isotropic; that is, the same etch rate is present at different planes.[30] The HF acidic etching is improved by the addition of HNO_3,[35] and it produces some pores on the silicon surface. In the Pt-assisted acidic etching, Pt particles are used to adjust the extent of HF etching through a local galvanic cell mechanism,[36] and Pt particles may also act as etch masks for short-time HF etching. Thus, the thick or thin Pt-assisted acidic etching would be expected to produce the porous silicon surfaces with different roughnesses.

Composition of FODMS-Modified Porous Silicon Surfaces. Surface chemical composition affects the surface hydrophobicity greatly. Here, we introduce a self-assembled monolayer of FODMS molecules with low surface energy to the obtained porous silicon surfaces. XPS has been proven to be a powerful tool to investigate the composition and structure of self-assembled monolayers. The typical XPS spectra of a bare porous silicon surface without FODMS treatment and FODMS-modified porous silicon surfaces are shown in Figure 2. As seen, the spectrum of Figure 2(1) for the bare porous silicon surface shows the presence of Si2s, Si2p, C1s, O1s, and O(A). Upon modification with FODMS, the new peaks for F1s at 689.0 eV and F(A) at 835.0 eV appear in the spectrum of Figure 2(2). This supports that the FODMS molecules have been successfully introduced onto the porous silicon surfaces.

To get further information on the surface composition of the FODMS-modified porous silicon surfaces, high resolution XPS data for C and Pt elements are also collected, which are shown in Figure 3. There are four peaks arising from C1s, as presented in Figure 3a. The peaks at 284.6, 291.3, and 293.6 eV can be

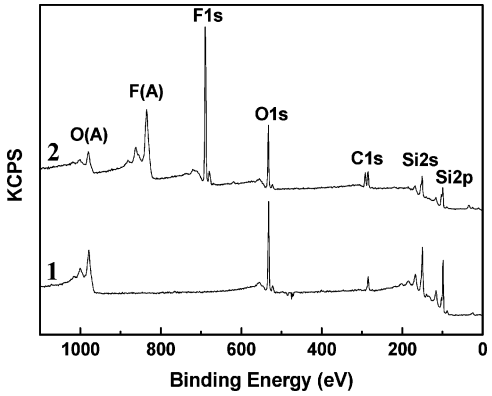

Figure 2. Typical XPS survey spectra for (1) the bare porous silicon surface and (2) FODMS-modified porous silicon surfaces.

assigned to CH_2, CF_2, and CF_3 groups, respectively, while the peak centered at 285.9 eV may originate from the unhydrolyzed methoxy group ($O-CH_3$). This also proves the successful introduction of FODMS molecules to the porous silicon surfaces. Moreover, a trace amount of Pt has been detected for the porous silicon surfaces produced by thick or thin Pt-assisted acidic etching, as shown by the spectrum of Figure 3b. This indicates that most of the Pt particles have been removed off the surfaces during the etching process.

Surface Hydrophobicity. As seen from the inset images of Figure 1, the equilibrium water contact angles of the FODMS-modified porous silicon surfaces produced by different etching methods are 116, 153, 161, and 155° for alkaline etching, acidic etching, thick Pt-assisted acidic etching, and thin Pt-assisted acidic etching, respectively. Evidently, except for the porous silicon surface produced by alkaline etching, all of the other three surfaces show superhydrophobicity. During experiments, if the latter three surfaces are tilted slightly, a water drop tends to roll off.

It is well-known that the air trapped in the solid surface is very important to hydrophobicity, because the water contact angle of air is regarded to be 180°.[1] Cassie and Baxter have proposed the following equation to express the contact angle on a composite surface (θ_r):[37]

$$\cos \theta_r = f_1 \cos \theta - f_2 \quad (3)$$

Here, θ_r and θ are the contact angles of water on the FODMS-modified porous silicon surfaces and on the FODMS-modified smooth silicon surface, respectively, and f_1 and f_2 are the fractions of solid surfaces and air in contact with water, respectively. It is assumed that $f_1 + f_2 = 1$. The water contact angle of the FODMS-modified smooth silicon surface is ~105°, as reported previously,[28] which is used as θ in the calculation. Thus, for the four FODMS-modified porous silicon surfaces, the fractions of air in the surfaces can be calculated from eq 3. The results are shown in Table 1. As seen, the increase in contact angles corresponds to the increase in f_2 values. This indicates that the achievement of superhydrophobicity is mainly a result of the air trapped in the surface. The lowest f_2 value is found for the porous silicon surface produced by alkaline etching. The reason may be that the water can penetrate the space between the pyramid structures and wet the underlying areas of the surface due to the smooth sides and small heights of the pyramids. The largest f_2 value of 0.926 for the porous silicon surface produced by thick Pt-assisted acidic etching indicates that the micro- and nanoscale binary structures bear the largest roughness.

TABLE 1: Calculated Fractions of Solid Surfaces (f_1) and Air (f_2) in Contact with Water

	alkaline etching	acidic etching	thick Pt-assisted acidic etching	thin Pt-assisted acidic etching
f_1	0.758	0.147	0.074	0.126
f_2	0.242	0.853	0.926	0.874

Surface Reflectivity. An ideal antireflective coating satisfies the following conditions: $n_c = (n_a n_s)^{0.5}$, where n_c, n_a, and n_s are the refractive indices of the coating material, air, and substrate, respectively; and the surface pore size is smaller than the quarter-wavelength of the incident light.[38] To reach efficient antireflection, n_c must be between 1.2 and 1.3.[14,17] However, the lowest refractive index of the available materials is about 1.35.[38] One solution to lower the n_c value is to use appropriately designed porous surface structures to introduce air into the surfaces because the refractive index of air is only 1. Nevertheless, although a rough surface is crucial for getting a porous silicon surface with both superhydrophobicity and high antireflectivity, antireflectivity seems to be competitive with the superhydrophobicity, since a surface with increasing roughness also becomes more a source for light scattering.

Figure 4 shows the reflection spectra of the bare silicon surface and the porous silicon surfaces made by the four etching methods. As seen, the porous silicon surfaces produced by alkaline etching and acidic etching cannot reduce the reflectance effectively, whose reflectance values are only about 5 and 10% lower than the bare silicon surface. A much lower reflectance has been found for the porous silicon surface by thick Pt-assisted acidic etching, which is averaged to be about 12% in the visible wavelength range and a slightly higher value in the ultraviolet wavelength range. Furthermore, the lowest reflectance value averaged to be about 3% over the whole photon wavelength spanning 300−800 nm can be reached by the thin Pt-assisted acidic etching.

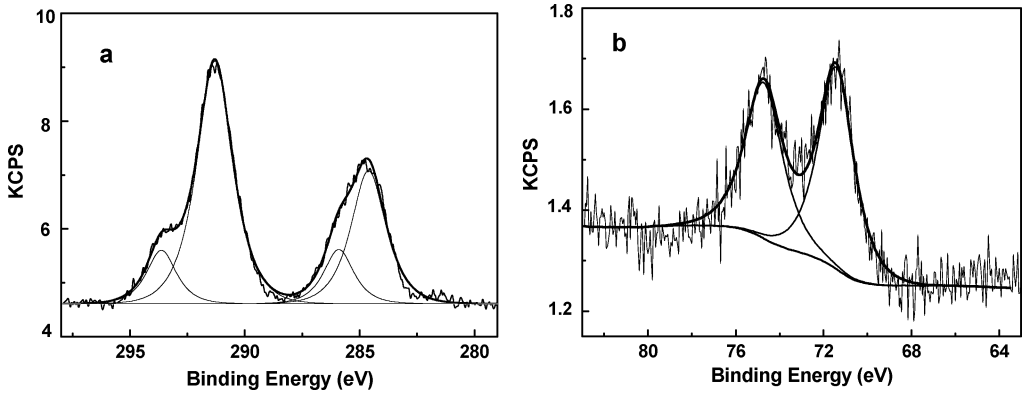

Figure 3. XPS spectra for FODMS-modified porous silicon surfaces: (a) C1s spectrum; (b) Pt4f spectrum.

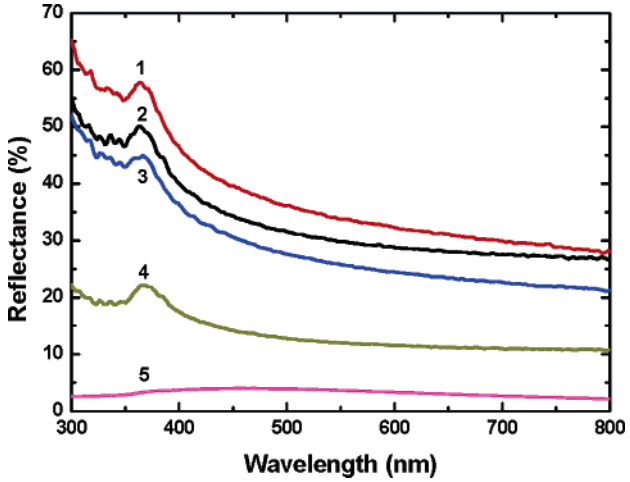

Figure 4. Reflection spectra of the bare silicon surface and the porous silicon surfaces produced by different etching methods: (1) bare silicon surface; (2) acidic etching; (3) alkaline etching; (4) thick Pt-assisted acidic etching; (5) thin Pt-assisted acidic etching.

The different antireflection efficiencies of the four porous silicon surfaces are thought to be closely related to their surface morphologies. It is deduced that the micrometer-sized pyramids and huge pores on the two surfaces produced by alkaline and acidic etching are too big and they cause intense light scattering; thus, high antireflection efficiency cannot be obtained. Nevertheless, the two spongelike surfaces produced by thick and thin Pt-assisted acidic etching bear many deep holes and silicon particles whose sizes are at wide ranges. The highly porous structures can introduce a great amount of air into the surfaces to reduce the refractive index. Thus, both of the surfaces give the much lower reflectance values. However, the microscale structures presented on the porous silicon surface produced by the thick Pt-assisted acidic etching would cause light scattering to a certain extent. Thus, this surface can only reach a much lower but not the lowest reflectance. Differently, the smaller nano- and submicroscale roughness of the surface produced by the thin Pt-assisted acidic etching can avoid intense light scattering. Thus, this surface owns the highest antireflectivity efficiency over a wider wavelength range.

Conclusions

In summary, four different porous silicon surfaces are fabricated using alkaline etching, acidic etching, thick Pt-assisted acidic etching, and thin Pt-assisted acidic etching. After being modified with FODMS, the wettability and reflectivity of these surfaces strongly depend on the etching method and the resultant surface morphology. All of the four porous silicon surfaces produced by different etching methods can reduce reflectance, but their efficiency differs greatly. Except for the alkaline etching, the porous silicon surfaces produced by the other three etching methods can reach superhydrophobicity after fluoroalkylsilane modification. Moreover, high antireflectivity has been found for the two porous silicon surfaces produced by thick and thin Pt-assisted acidic etching. Especially, the surface by thin Pt-assisted acidic etching can reach a very low reflectance over a wide wavelength range. The achievement of both high antireflectivity and superhydrophobicity are thought to be generated by the micro-, submicro-, and nanoscale roughness on the porous silicon surfaces, which are effective to avoid intense light scattering and ensure enough air is being trapped in the surfaces. The porous silicon surface with both high antireflectivity and superhydrophobicity may promise potential applications in the construction of high efficiency, silicon-based solar cells with self-cleaning function.

Acknowledgment. We are grateful for financial support from the National Science Foundation of China (20233010, 20473101) and National Basic Research Program of China (2005CB221300).

References and Notes

(1) Jiang, L.; Zhao, Y.; Zhai, J. *Angew. Chem., Int. Ed*. **2004**, *43*, 4338−4341.
(2) Furstner, R.; Barthlott, W.; Neinhuis, C.; Walzel, P. *Langmuir* **2005**, *21*, 956−961.
(3) Patankar, N. A. *Langmuir* **2004**, *20*, 8209−8213.
(4) Zhai, L.; Cebeci, F. C.; Cohen, R. E.; Rubner, M. F. *Nano Lett.* **2004**, *4*, 1349−1353.
(5) Feng, L.; Li, S. H.; Li, H. J.; Zhai, J.; Song, Y. L.; Jiang, L.; Zhu, D. B. *Angew. Chem., Int. Ed.* **2002**, *41*, 1221−1223.
(6) Feng, L.; Li, S. H.; Li, Y. S.; Li, H. J.; Zhang, L. J.; Zhai, J.; Song, Y. L.; Liu B. Q.; Jiang, L.; Zhu, D. B. *Adv. Mater*. **2002**, *14*, 1857−1860.
(7) Zhang, X.; Shi, F.; Yu, X.; Liu, H.; Fu, Y.; Wang, Z. Q.; Jiang, L.; Li, X. Y. *J. Am. Chem. Soc*. **2004**, *126*, 3064−3065.
(8) Feng X. J.; Feng L.; Jin M. H.; Zhai J.; Jiang L.; Zhu, D. B. *J. Am. Chem. Soc.* **2004**, *126*, 62−63.
(9) Sun, T.; Wang, G.; Liu, H.; Feng, L.; Jiang, L.; Zhu, D. *J. Am. Chem. Soc.* **2003**, *125*, 14996−14997.
(10) Onda, T.; Shibuichi, N.; Satoh, N.; Tsujii, K. *Langmuir* **1996**, *12*, 2125−2127.
(11) Erbil, H. Y.; Demirel, A. L.; Avci, Y.; Mert, O. *Science* **2003**, *299*, 1377−1380.
(12) Nakajima, A.; Fujishima, A.; Hashimoto, K.; Watanabe, T. *Adv. Mater*. **1999**, *11*, 1365−1368.
(13) Ibn-Elhaj, M.; Schadt, M. *Nature* **2001**, *410*, 796−799.
(14) Hiller, J.; Mendelsohn, J. D.; Rubner, M. F. *Nat. Mater*. **2002**, *1*, 59−63.
(15) Yabu, H.; Shimomura, M. *Chem. Mater*. **2005**, *17*, 5231−5234.
(16) Shang, H. M.; Wang, Y.; Limmer, S. J.; Chou, T. P.; Takahashi, K.; Cao, G. Z. *Thin Solid Films* **2005**, *472*, 37−43.
(17) Hattori, H. *Adv. Mater*. **2001**, *13*, 51−54.
(18) Koo, H. Y.; Yi, D. K.; Yoo, S. J.; Kim, D.-Y. *Adv. Mater*. **2004**, *16*, 274−277.
(19) Park, M. S.; Lee, Y.; Kim, J. K. *Chem. Mater*. **2005**, *17*, 3944−3950.
(20) Drabczyk, K.; Panek, P.; Lipiñski, M. *Sol. Energy Mater. Sol. Cells* **2003**, *76*, 545−551.
(21) Schirone, L.; Sotgiu, G.; Califano, F. P. *Thin Solid Films* **1997**, *297*, 296−298.
(22) Kawakami, K.; Fujii, T.; Yae, S.; Nakato, Y. *J. Phys. Chem. B* **1997**, *101*, 4508−4513.
(23) Nakajima, A.; Hashimoto, K.; Watanabe, T.; Takai, K.; Yamauchi, G.; Fujishima, A. *Langmuir* **2000**, *16*, 7044−7047.
(24) Zhang, X.-T.; Sato, O.; Taguchi, M.; Einaga, Y.; Murakami, T.; Fujishima, A. *Chem. Mater*. **2005**, *17*, 696−700.
(25) Tadanaga, K.; Katata, N.; Minami, T. *J. Am. Ceram. Soc.* **1997**, *80*, 1040−1042.
(26) Xu, Y.; Fan, W. H.; Li, Z. H.; Wu, D.; Sun, Y. H. *Appl. Opt*. **2003**, *42*, 108−112.
(27) Wang, X.; Li, Y.; Wang, J.; Wang, Y.; Ye, J.; Wang, Z.; Yan, H.; Zhang, J.; Thomas, R. K. *J. Phys. Chem. B* **2005**, *109*, 12850−12855.
(28) Song, X. Y.; Zhai, J.; Wang, Y. L.; Jiang, L. *J. Phys. Chem. B* **2005**, *109*, 4048−4052.
(29) Yuan, F.; Guo, Y.; Liang, Y.; Yan, Y.; Fu, H.; Cheng, K.; Luo, X. *J. Mater. Proc. Technol*. **2004**, *149*, 567−572.
(30) Robbins, H.; Schwartz, B. *J. Electrochem. Soc.* **1959**, *106*, 505−508.
(31) Rappich, H.; Lewerenz, H. J.; Gerischer, H. J. *J. Electrochem. Soc.* **1993**, *140*, L187−L189.
(32) Seidal, H.; Csepregi, L.; Heuberger, A.; Baumgartel, H. *J. Electrochem. Soc.* **1990**, *137*, 3612−3626.
(33) Zubel, I.; Barycka, I. *Sens. Actuators, A* **1998**, *70*, 250−259.
(34) Divan, R.; Moldovan, N.; Camon, H. *Sens. Actuators, A* **1999**, *74*, 18−23.
(35) Henssge, A.; Acker, J.; Müller, C. *Talanta* **2006**, *68*, 581−585.
(36) Li, X.; Bohn, P. W. *Appl. Phys. Lett*. **2000**, *77*, 2572−2574.
(37) Cassie, A. B. D.; Baxter, S. *Trans. Faraday Soc*. **1944**, *40*, 546−551.
(38) Macleod, H. A. *Thin-Film Optical Filters*; Elsevier: New York, 1969.